

Reactions of a Ru(II) Phenyl Complex with Substrates that Possess C–N or C–O Multiple Bonds: C–C Bond Formation, N–H Bond Cleavage, and Decarbonylation Reactions

John P. Lee,[†] Karl A. Pittard,[†] Nathan J. DeYonker,[‡] Thomas R. Cundari,[‡]
T. Brent Gunnoe,^{*,†} and Jeffrey L. Petersen[§]

Department of Chemistry, North Carolina State University, Raleigh, North Carolina 27695-8204,
Center for Advanced Scientific Computing and Modeling (CASCaM), Department of Chemistry,
University of North Texas, Box 305070, Denton, Texas 76203-5070, and C. Eugene Bennett Department of
Chemistry, West Virginia University, Morgantown, West Virginia 26506-6045

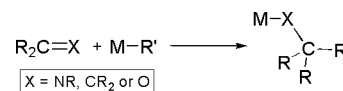
Received November 10, 2005

The Ru(II) phenyl complex TpRu(CO)(NCMe)(Ph) (**1**) (Tp = hydridotris(pyrazolyl)borate) reacts with carbodiimides to yield amidinate complexes that result from C–C bond formation between the phenyl ligand and the carbodiimide carbon. Complex **1** and *N*-methylacetamide react to produce benzene and the amidate complex TpRu(CO){(*N,O*-OC(Me)N(Me))} (**4**). The reaction of complex **1** with C≡N(*t*Bu) yields TpRu(CO){C≡N(*t*Bu)}(Ph) (**5**), and heating a solution of PMe₃ and **5** results in the observation of an equilibrium with the product of isonitrile insertion TpRu(CO){C(Ph)=N^{*t*}Bu}(PMe₃) (**6**) ($\Delta H = +9(1)$ kcal/mol and $\Delta S = +20(3)$ eu). The reaction of **1** with aromatic aldehydes at elevated temperatures results in C–H activation and decarbonylation of the aldehyde to produce TpRu(CO)₂(Ar) (Ar = phenyl or *p*-tolyl) and free benzene. DFT calculations have been incorporated to study coordination and insertion reactions of ethylene, methyleneimine, formaldehyde, HN=C=NH, and C≡NH into the Ru–Ph bond of the model fragment (Tab)Ru(CO)(Ph) (Tab = tris(azo)borate). In addition, the energetics of Ru-mediated decarbonylation of formaldehyde have been calculated.

Introduction

Insertions of substrates that possess multiple bonds into transition metal alkyl, aryl, or hydride bonds provide a fundamental class of reaction that is central to many catalytic cycles. Although insertions of olefin C=C bonds into metal–alkyl, –acyl, –hydride, or –aryl bonds have substantial precedent,^{1,2} examples of direct observation of insertion reactions involving C–O or C–N multiple bonds of imines, ketones, aldehydes, or related substrates (with the exception of CO and CO₂) are scarce relative to analogous insertions of olefins (Scheme 1).^{3–16} This is especially true for late transition metal

Scheme 1. Insertion of Olefin, Imine, or Carbonyl Group into M–R' Bond to Produce C–C and M–X Bonds



systems, while examples of insertion reactions of C–O or C–N multiple bonds (especially involving the formation of metallacycles) are more prevalent for early transition metal systems.^{17–21}

A potential explanation for the scarcity of insertion reactions involving metal–carbon bonds and substrates with C–O or C–N multiple bonds is the difference in bond dissociation energies (BDEs) for the unsaturated compounds. However, since insertion reactions of C=X bonds into M–R bonds result in the transformation of C=X double bonds into C–X single bonds, consideration of the *relative* BDEs of C=X (X = C, O, or N) double bonds and C–X single bonds perhaps provides a more complete picture, and rationalizing reactivity on the basis of typical BDEs for C–C, C–O, and C–N multiple bonds may be too simplistic. Another factor that potentially exacerbates

* To whom correspondence should be addressed. E-mail: brent_gunnoe@ncsu.edu.

[†] North Carolina State University.

[‡] University of North Texas.

[§] West Virginia University.

(1) Collman, J. P.; Hegedus, L. S.; Norton, J. R.; Finke, R. G. *Principles and Applications of Organotransition Metal Chemistry*; University Science: Mill Valley, CA, 1987.

(2) Crabtree, R. H. *The Organometallic Chemistry of the Transition Metals*, 2nd ed.; John Wiley and Sons: New York, 1994.

(3) Krug, C.; Hartwig, J. F. *J. Am. Chem. Soc.* **2004**, *126*, 2694–2695.

(4) Krug, C.; Hartwig, J. F. *J. Am. Chem. Soc.* **2002**, *124*, 1674–1679.

(5) Fryzuk, M. D.; Piers, W. E. *Organometallics* **1990**, *9*, 986–998.

(6) Alelyunas, Y. W.; Jordan, R. F.; Echols, S. F.; Borkowsky, S. L.; Bradley, P. K. *Organometallics* **1991**, *10*, 1406–1416.

(7) Braunstein, P.; Matt, D.; Nobel, D. *Chem. Rev.* **1988**, *88*, 747–764.

(8) Jessop, P. G.; Ikariya, T.; Noyori, R. *Chem. Rev.* **1995**, *95*, 259–272.

(9) Krug, C.; Hartwig, J. F. *Organometallics* **2004**, *23*, 4594–4607.

(10) Kacker, S.; Kim, J. S.; Sen, A. *Angew. Chem., Int. Ed.* **1998**, *37*, 1251–1253.

(11) Baar, C. R.; Jennings, M. C.; Vittal, J. J.; Puddephatt, R. J. *Organometallics* **2000**, *19*, 4150–4158.

(12) Cavallo, L. *J. Am. Chem. Soc.* **1999**, *121*, 4238–4241.

(13) Davis, J. L.; Arndtsen, B. A. *Organometallics* **2000**, *19*, 4657–4659.

(14) Dghaym, R. D.; Yaccato, K. J.; Arndtsen, B. A. *Organometallics* **1998**, *17*, 4–6.

(15) Hartwig, J. F.; Andersen, R. A.; Bergman, R. G. *J. Am. Chem. Soc.* **1989**, *111*, 2717–2719.

(16) Carmona, E.; Gutiérrez-Puebla, E.; Marín, J. M.; Monge, A.; Paneque, M.; Poveda, M. L.; Ruiz, C. *J. Am. Chem. Soc.* **1989**, *111*, 2883–2891.

(17) Erker, G.; Kehr, G.; Fröhlich, R. *Adv. Organomet. Chem.* **2004**, *51*, 109–162.

(18) Jordan, R. F. *Adv. Organomet. Chem.* **1991**, *32*, 325–387.

(19) Tikkanen, W. R.; Petersen, J. L. *Organometallics* **1984**, *3*, 1651–1655.

(20) Zhao, C.; Yan, J.; Zhenfeng, X. *J. Org. Chem.* **2003**, *68*, 4355–4360.

(21) Gordon, G. J.; Whitby, R. J. *Chem. Commun.* **1997**, 1321–1322.

the predisposition against C=O and C=N insertion (relative to C=C insertion) is the resulting M–X (X = N or O) BDEs. For late transition metal systems, it has been demonstrated that M–C(sp³) BDEs can be greater than M–NR₂ BDEs and of similar magnitude to M–OR BDEs.^{22,23} Thus, if it is assumed that the C–C BDEs of the inserted products are of similar magnitude, the enthalpic factors that dictate the relative propensity for C=X insertion into M–C bonds are the difference in C=X/C–X BDEs and the relative M–X BDEs making general predictions for classes of substrates complex. Another potential difference between insertion reactions involving C=X bonds and those involving C=C bonds is the access to both monohapto and dihapto coordination modes for the former while the latter is restricted to dihapto coordination.

An increased understanding of the factors that dictate the course of potential insertion reactions involving C–N or C–O multiple bonds could lead to the development of new pathways for carbon–carbon bond formation. For example, several advances in catalytic transformations of aromatic carbon–hydrogen bonds have been recently reported.^{24–43} Due in part to the atom economical nature of these transformations, the addition of carbon–hydrogen bonds across multiple bonds has emerged as a promising area within organic synthesis.^{29,44–53}

(22) Bryndza, H. E.; Domaille, P. J.; Tam, W.; Fong, L. K.; Paciello, R. A.; Bercaw, J. E. *Polyhedron* **1988**, *7*, 1441–1452.

(23) Bryndza, H. E.; Fong, L. K.; Paciello, R. A.; Tam, W.; Bercaw, J. E. *J. Am. Chem. Soc.* **1987**, *109*, 1444–1456.

(24) Rittleng, V.; Sirlin, C.; Pfeffer, M. *Chem. Rev.* **2002**, *102*, 1731–1769.

(25) Dyker, G. *Angew. Chem., Int. Ed.* **1999**, *38*, 1698–1712.

(26) Goldberg, K. I.; Goldman, A. S. *Activation and Functionalization of C–H Bonds*; American Chemical Society: Washington, DC, 2004; Vol. 885.

(27) Kakiuchi, F.; Murai, S. *Acc. Chem. Res.* **2002**, *35*, 826–834.

(28) Kakiuchi, F.; Murai, S. In *Topics in Organometallic Chemistry*; Murai, S., Ed.; Springer: Berlin, 1999; Vol. 3, pp 47–79.

(29) Jia, C.; Kitamura, T.; Fujiwara, Y. *Acc. Chem. Res.* **2001**, *34*, 633–639.

(30) Kakiuchi, F.; Chatani, N. *Adv. Synth. Catal.* **2003**, *345*, 1077–1101.

(31) Hennessy, E. J.; Buchwald, S. L. *J. Am. Chem. Soc.* **2003**, *125*, 12084–12085.

(32) Lenges, C. P.; Brookhart, M. *J. Am. Chem. Soc.* **1999**, *121*, 6616–6623.

(33) Weissman, H.; Song, X.; Milstein, D. *J. Am. Chem. Soc.* **2001**, *123*, 337–338.

(34) Thalji, R. K.; Ahrendt, K. A.; Bergman, R. G.; Ellman, J. A. *J. Am. Chem. Soc.* **2001**, *123*, 9692–9693.

(35) Tan, K. L.; Bergman, R. G.; Ellman, J. A. *J. Am. Chem. Soc.* **2001**, *123*, 2685–2686.

(36) Sezen, B.; Sames, D. *J. Am. Chem. Soc.* **2003**, *125*, 5274–5275.

(37) Jordan, R. F.; Taylor, D. F. *J. Am. Chem. Soc.* **1989**, *111*, 778–779.

(38) Cho, J.-Y.; Tse, M. K.; Holmes, D.; Maleczka, R. E.; Smith, M. R., III. *Science* **2002**, *295*, 305–308.

(39) Chen, H.; Schlecht, S.; Semple, T. C.; Hartwig, J. F. *Science* **2000**, *287*, 1995–1997.

(40) Stahl, S. S.; Labinger, J. A.; Bercaw, J. E. *Angew. Chem., Int. Ed.* **1998**, *37*, 2180–2192.

(41) Shilov, A. E.; Shul'pin, G. B. *Activation and Catalytic Reactions of Saturated Hydrocarbons in the Presence of Metal Complexes*; Kluwer Academic Publishers: Dordrecht, 2000; Vol. 21.

(42) Labinger, J. A.; Bercaw, J. E. *Nature* **2002**, *417*, 507–514.

(43) Sen, A. *Acc. Chem. Res.* **1998**, *31*, 550–557.

(44) Matsumoto, T.; Taube, D. J.; Periana, R. A.; Taube, H.; Yoshida, H. *J. Am. Chem. Soc.* **2000**, *122*, 7414–7415.

(45) Matsumoto, T.; Periana, R. A.; Taube, D. J.; Yoshida, H. *J. Mol. Catal. A: Chemical* **2002**, *180*, 1–18.

(46) Oxgaard, J.; Muller, R. P.; Goddard, W. A., III; Periana, R. A. *J. Am. Chem. Soc.* **2004**, *126*, 352–363.

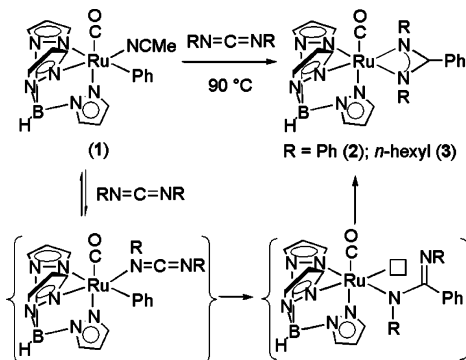
(47) Oxgaard, J.; Periana, R. A.; Goddard III, W. A. *J. Am. Chem. Soc.* **2004**, *126*, 11658–11665.

(48) Periana, R. A.; Liu, X. Y.; Bhalla, G. *Chem. Commun.* **2002**, *24*, 3000–3001.

(49) Shi, Z.; He, C. *J. Org. Chem.* **2004**, *69*, 3669–3671.

(50) Pastine, S. J.; Youn, S. W.; Sames, D. *Org. Lett.* **2003**, *5*, 1055–1058.

Scheme 2. Possible Reaction Pathway for the Formation of Amidinate Complexes 2 and 3



Our group has been exploring the utilization of Ru(II) complexes for the catalytic hydroarylation of olefins.^{54–56} For example, TpRu(CO)(NCMe)(Ph) (**1**) (Tp = hydridotris(pyrazolyl)borate) catalyzes the hydroarylation of ethylene and α -olefins, and heteroaryl systems of the type TpRu(CO)(NCMe)(Ar) (Ar = 2-thienyl or 2-furyl) catalyze the regioselective addition of furan or thiophene 2-position C–H bonds across the C=C bond of ethylene. To date, our studies have focused on the hydroarylation of olefins; however, extension of the C–C bond-forming step to unsaturated substrates other than olefins would ultimately expand the synthetic utility of such reactions. Herein, we report on experimental and computational studies that probe reactions of substrates that possess C–O or C–N multiple bonds with the Ru(II) phenyl complex TpRu(CO)(NCMe)(Ph) (**1**).

Results and Discussion

Experimental Studies. The reaction of TpRu(CO)(NCMe)-(Ph) (**1**) with either *N,N*-diphenylcarbodiimide or *N,N*-di-*n*-hexylcarbodiimide results in the formation of the corresponding Ru(II) amidinate complexes TpRu(CO){*N,N*-(Ph)NC(Ph)N(Ph)} (**2**) and TpRu(CO){*N,N*-(*n*-hexyl)NC(Ph)N(*n*-hexyl)} (**3**), respectively (Scheme 2). The amidinate complexes **2** and **3** are characterized by $\nu_{\text{CO}} = 1937$ and 1929 cm^{-1} , respectively, in their IR spectra, and ¹H and ¹³C NMR spectra are consistent with C_s molecular symmetry. Complexes **2** and **3** are the only observable species by NMR spectroscopy (in crude reaction mixtures) and are isolated pure in 39% and 58% yield, respectively, after workup. The formation of amidinate complexes is consistent with the net insertion of C=N bonds of the carbodiimides into the Ru–Ph bond of the {TpRu(CO)(Ph)} fragment followed by chelation to form the amidinate moiety (Scheme 2). Insertions of carbodiimides into lanthanide, main group, and electron-deficient early transition metal M–R bonds have been reported.^{57–62}

(51) Youn, S. W.; Pastine, S. J.; Sames, D. *Org. Lett.* **2004**, *6*, 581–584.

(52) Pastine, S. J.; Youn, S. W.; Sames, D. *Tetrahedron* **2003**, *59*, 8859–8868.

(53) Goj, L. A.; Gunnoe, T. B. *Curr. Org. Chem.* **2005**, *9*, 671–685.

(54) Lail, M.; Arrowood, B. N.; Gunnoe, T. B. *J. Am. Chem. Soc.* **2003**, *125*, 7506–7507.

(55) Lail, M.; Bell, C. M.; Conner, D.; Cundari, T. R.; Gunnoe, T. B.; Petersen, J. L. *Organometallics* **2004**, *23*, 5007–5020.

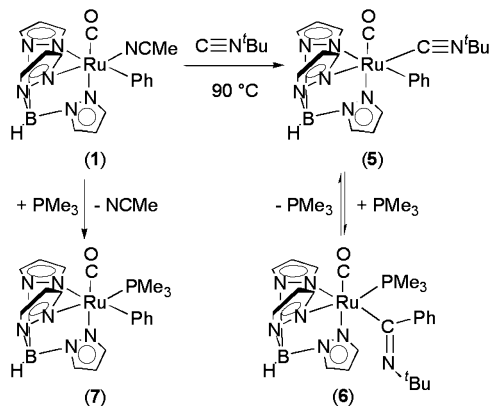
(56) Pittard, K. A.; Lee, J. P.; Cundari, T. R.; Gunnoe, T. B.; Petersen, J. L. *Organometallics* **2004**, *23*, 5514–5523.

(57) Rowley, C. N.; DiLabio, G. A.; Barry, S. T. *Inorg. Chem.* **2005**, *44*, 1983–1991.

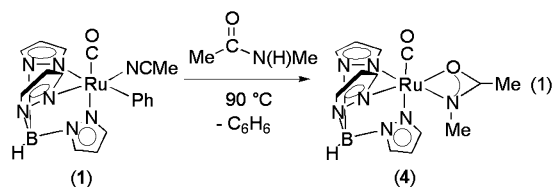
(58) Zhang, J.; Ruan, R.; Shao, Z.; Cai, R.; Weng, L.; Zhou, X. *Organometallics* **2002**, *21*, 1420–1424.

(59) Li, M.-D.; Chang, C.-C.; Wang, Y.; Lee, G.-H. *Organometallics* **1996**, *15*, 2571–2574.

Scheme 3. Formation of TpRu(CO)(CN^{*t*}Bu)(Ph) (5), Observation of Insertion of Isonitrile into the Ru–Phenyl Ligand, and Preparation of TpRu(CO)(Ph)(PMe₃) (7)



Heating a solution of complex 1 and *N*-methylacetamide results in the production of free benzene and the amidate complex TpRu(CO){(*N,O*-OC(Me)N(Me))} (4) as the only observable TpRu species in the ¹H NMR spectra of crude reaction mixtures (eq 1). The production of benzene has been



confirmed by NMR spectroscopy of reactions run in deuterated solvents and NMR tubes. Complex 4 could not be separated from the excess *N*-methylacetamide (see Experimental Section). Rather than insertion of C=O, complex 1 reacts with *N*-methylacetamide to initiate N–H bond cleavage and produce benzene and complex 4. Reports of reactions with transition metal systems that involve activation of carboxamide N–H bonds are relatively rare.^{63,64} Heating a solution of 1 and *N,N*-dimethylacetamide (which lacks an N–H bond) results in decomposition to NMR-silent ruthenium complexes; similar observations (i.e., decomposition of 1) are made when complex 1 is heated in neat C₆D₆.⁵⁵

The reaction of TpRu(CO)(NCMe)(Ph) (1) with CN^{*t*}Bu forms the ligand-substitution product TpRu(CO)(CN^{*t*}Bu)(Ph) (5) in quantitative yield by ¹H NMR spectroscopy and 33% isolated yield after workup (Scheme 3). Neither extended thermolysis nor photolysis of complex 5 in C₆D₆ or CD₃CN affords isonitrile insertion into the Ru–Ph bond to form TpRu(CO){C(Ph)=N^{*t*}Bu}(L) (L = CD₃CN or C₆D₆). Assuming that L = benzene or acetonitrile might result in thermodynamically disfavored insertion processes; complex 5 was heated to 100 °C in benzene in the presence of PMe₃. Under these conditions, the formation of TpRu(CO){C(Ph)=N^{*t*}Bu}(PMe₃) (6) in equilibrium with complex 5 and free PMe₃ is observed (Scheme 3). Salient characterization features of 6 include a resonance at 11.0

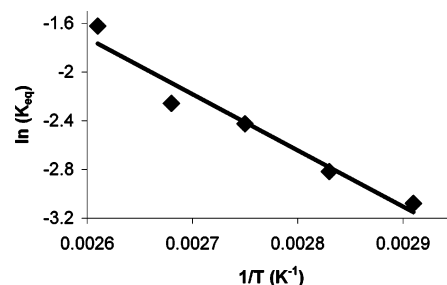
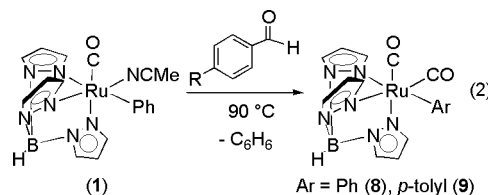


Figure 1. Plot of ln(*K*_{eq}) versus 1/*T* (van't Hoff plot) for the equilibrium between complex 5/PMe₃ and complex 6 (*R*² = 0.96).

ppm in the ³¹P NMR spectrum, a singlet at 1.21 ppm, and a doublet (²*J*_{PH} = 10 Hz) at 1.27 ppm in the ¹H NMR spectrum assigned as the resonances due to the ^{*t*}Bu group and the coordinated PMe₃, respectively. In addition, following the transformation by IR spectroscopy reveals a new CO absorption at 1927 cm⁻¹ (*ν*_{CO} = 1952 cm⁻¹ for 5) and a decrease in the intensity of the absorption due to the isonitrile C≡N bond. The changes observed by IR spectroscopy are consistent with isonitrile insertion into the Ru–phenyl bond and are inconsistent with insertion of the CO ligand. The independent preparation of TpRu(CO)(Ph)(PMe₃) (7) verified that the reaction of TpRu(CO)(CN^{*t*}Bu)(Ph) (5) and PMe₃ does not produce complex 7 (Scheme 3). Insertion of isonitriles into metal–alkyl or –aryl bonds have been previously observed or proposed to occur in catalytic cycles.^{65–72} Removal of the volatiles from the mixture of 5, 6, and PMe₃ in C₆D₆ (including all free PMe₃) and dissolution of the nonvolatiles in C₆D₆ result in the conversion of 6 back to free PMe₃ and complex 5 as determined by NMR spectroscopy. Determination of *K*_{eq} at temperatures ranging from 70 to 110 °C allowed a linear van't Hoff plot for the equilibrium between complex 5/PMe₃ and complex 6 (Figure 1). The van't Hoff analysis yields an estimated Δ*H* = +9(1) kcal/mol and Δ*S* = +20(3) eu. Thus, the insertion is disfavored by change in enthalpy, supporting the notion that a relatively strong M–L BDE is required to trap the insertion product and allow observation of this species. Cardaci et al. have elucidated the thermodynamic parameters for insertion of CN^{*t*}Bu into Fe(II) methyl bonds of cationic octahedral complexes to yield η²-coordinated iminoacyl ligands.⁷³ For these systems, Δ*H* ranged from –1.6 to –1.9 kcal/mol with Δ*S* of –5 to –7 eu.

The reaction of complex 1 and benzaldehyde at 90 °C results in net decarbonylation to produce TpRu(CO)₂(Ph) (8) and



benzene (eq 2). Consistent with the formation of a cis-dicarbonyl

(60) Jayaratne, K. C.; Sita, L. R. *J. Am. Chem. Soc.* **2000**, *122*, 958–959.

(61) Koterwas, L. A.; Fettingner, J. C.; Sita, L. R. *Organometallics* **1999**, *18*, 4183–4190.

(62) Coles, M. P.; Swenson, D. C.; Jordan, R. F.; Young, J., R. J. *Organometallics* **1998**, *17*, 4042–4048.

(63) Schaad, D. R.; Landis, C. R. *Organometallics* **1992**, *11*, 2024–2029.

(64) Schaad, D. R.; Landis, C. R. *J. Am. Chem. Soc.* **1990**, *112*, 1628–1629.

(65) Jones, W. D.; Foster, G. P.; Putinas, J. M. *J. Am. Chem. Soc.* **1987**, *109*, 5047–5048.

(66) Jones, W. D.; Hessel, E. T. *Organometallics* **1990**, *9*, 718–727.

(67) Hsu, G. C.; Kosar, W. P.; Jones, W. D. *Organometallics* **1994**, *13*, 385–396.

(68) Jones, W. D.; Feher, F. J. *Organometallics* **1983**, *2*, 686–687.

(69) Tanaka, M.; Sakakura, T.; Tokunaga, Y.; Sodeyama, T. *Chem. Lett.* **1987**, 2373–2374.

(70) Motz, P. L.; Alexander, J. J.; Ho, D. M. *Organometallics* **1989**, *8*, 2589–2601.

(71) Durfee, L. D.; Rothwell, I. P. *Chem. Rev.* **1988**, *88*, 1059–1079.

(72) Kloppenburg, L.; Petersen, J. L. *Organometallics* **1997**, *16*, 3548–3556.

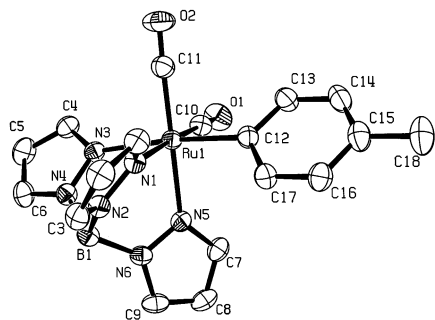


Figure 2. ORTEP (30% probability) of $\text{TpRu}(\text{CO})_2(p\text{-tolyl})$ (**9**) (hydrogen atoms have been omitted for clarity); selected bond lengths (\AA) and bond angles (deg): Ru1–C10 1.857(2); Ru1–C11 1.866(2); Ru1–C12 2.087(2); Ru1–N1 2.120(1); Ru1–N3 2.177(2); Ru1–N5 2.122(1); Ru1–C12–C13 124.7(2); C12–Ru1–C10 89.19(8); C12–Ru1–C11 89.71(8); N1–Ru1–N3 83.69(5); N1–Ru1–N5 85.08(5); N3–Ru1–N5 85.15(5); C12–Ru1–N3 172.50(6); Ru1–C10–O1 179.1(2); Ru1–C11–O2 178.2(2); C10–Ru1–C11 90.07(8).

complex, the IR spectrum of **8** reveals $\nu_{\text{CO}} = 2041$ and 1973 cm^{-1} . In addition, ^1H and ^{13}C NMR spectra reveal resonances consistent with C_s molecular symmetry, and the reaction of **8** with trimethylamine-*N*-oxide in acetonitrile (90°C) produces $\text{TpRu}(\text{CO})(\text{NCMe})(\text{Ph})$ (**1**). Both stoichiometric and catalytic metal-mediated decarbonylation reactions involving aldehydes have been reported.^{74–80}

For the conversion of $\text{TpRu}(\text{CO})(\text{NCMe})(\text{Ph})$ (**1**) and benzaldehyde to **8** and benzene, the production of benzene could potentially arise from the phenyl ligand of **1** or the phenyl group of the aldehyde. The reaction of **1** with *p*-tolualdehyde produces benzene and $\text{TpRu}(\text{CO})_2(p\text{-tolyl})$ (**9**) (eq 2). Consistent with a dicarbonyl complex, the IR spectrum of **9** exhibits $\nu_{\text{CO}} = 2039$ and 1971 cm^{-1} , and NMR spectra reveal resonances for the Tp ligand that are indicative of the presence of a mirror plane of symmetry. Slow evaporation of a pentane solution of **9** provided a single-crystal suitable for a solid-state X-ray diffraction study. The ORTEP of **9** is shown in Figure 2, and Table 1 presents selected crystallographic data and collection parameters. Regardless of the specific mechanism for C–H bond cleavage, the production of benzene clearly indicates that the pathway for decarbonylation involves the activation of an aldehyde C–H bond and subsequent (or simultaneous) C–H bond formation with the phenyl ligand of **1** to produce benzene. The aryl groups coordinated to Ru in the final dicarbonyl products $\text{TpRu}(\text{CO})_2(\text{Ar})$ (Ar) are derived from the aldehyde.

Attempted reaction of complex **1** with simple imines (e.g., *N*-benzylideneaniline and *N*-benzylidenemethylamine), acetone, or acetophenone results in decomposition without observation

(73) Bellachioma, G.; Cardaci, G.; Macchioni, A.; Zuccaccia, C. *J. Organomet. Chem.* **2000**, *593*–594, 119–126.

(74) Graham, P. M.; Mocella, C. J.; Sabat, M.; Harman, W. D. *Organometallics* **2005**, *24*, 911–919.

(75) Çelenligil-Çetin, R.; Watson, L. A.; Guo, C.; Foxman, B. M.; Ozerov, O. V. *Organometallics* **2005**, *24*, 186–189.

(76) Beck, C. M.; Rathmill, S. E.; Park, Y. J.; Chen, J.; Crabtree, R. H.; Liable-Sands, L. M.; Rheingold, A. L. *Organometallics* **1999**, *18*, 5311–5317.

(77) Abu-Hasanayn, F.; Goldman, M. E.; Goldman, A. S. *J. Am. Chem. Soc.* **1992**, *114*, 2520–2524.

(78) Morimoto, T.; Fujii, K.; Tsutsumi, K.; Kakiuchi, K. *J. Am. Chem. Soc.* **2002**, *124*, 3806–3807.

(79) Barrio, P.; Esteruelas, M. A.; Oñate, E. *Organometallics* **2004**, *23*, 1340–1348.

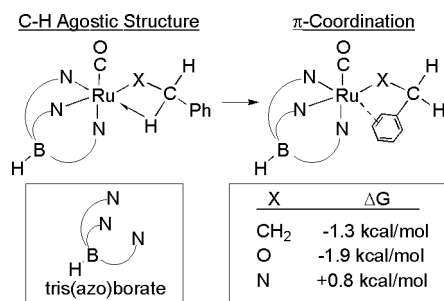
(80) Alaimo, P. J.; Arndtsen, B. A.; Bergman, R. G. *Organometallics* **2000**, *19*, 2130–2143.

Table 1. Selected Crystallographic Data and Collection Parameters for Complex **9**^a

complex	$\text{TpRu}(\text{CO})_2(p\text{-tolyl})$ (9)
empirical formula	$\text{C}_{18}\text{H}_{17}\text{N}_6\text{O}_2\text{BRu}$
fw	461.08
cryst syst	triclinic
space group	$P\bar{1}$
<i>a</i> , \AA	7.5379(4)
<i>b</i> , \AA	11.8576(6)
<i>c</i> , \AA	15.3064(7)
α , deg	79.215(1)
β , deg	78.105(1)
γ , deg	83.323(1)
$V(\text{\AA}^3)$	1310.78(11)
<i>Z</i>	2
D_{calcd} , g cm^{-3}	1.468
R1, wR2 ($I > 2\sigma(I)$)	0.0366, 0.0945
GOF	1.029

^a The crystallographic asymmetric unit also contains a disordered molecule of pentane and a disordered half-molecule of toluene.

Scheme 4. Stabilization of Insertion Products by Either a C–H Agostic Interaction or π -Interaction with the Phenyl Ring

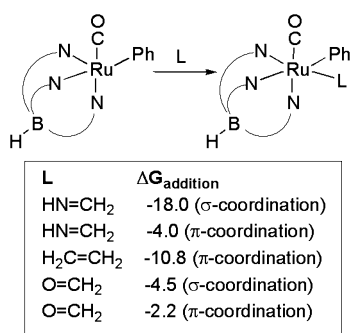


of Ru amido or alkoxide complexes, and the decomposition is analogous to that observed upon heating **1** in neat C_6D_6 .⁵⁵

Computational Studies of Insertion Reactions. Computational studies were performed to help delineate the details of possible insertion reactions of $\text{C}=\text{X}$ bonds into the Ru–Ph bond of complex **1**. Insertion reactions of five substrates have been studied and are compared herein: (1) ethylene, (2) $\text{HN}=\text{CH}_2$ (methyleneimine), (3) $\text{H}_2\text{C}=\text{O}$ (formaldehyde), (4) the parent carbodiimide $\text{HN}=\text{C}=\text{NH}$, and (5) the parent isonitrile $\text{C}\equiv\text{NH}$. In addition, the energetics for decarbonylation of $\text{H}_2\text{C}=\text{O}$ have been studied computationally. The “Tab” ligand (tris(azo)borate) and HCN were used to model Tp and MeCN, respectively. In previous research, Tab was shown to reproduce the structure and energetics of the full Tp models for C–H activation potential energy surfaces to within $\leq 2\%$ and ~ 2 kcal/mol, respectively.⁸¹ For all substrates other than ethylene, free energy changes for insertion reactions are reported relative to the most stable, i.e., monohapto-coordination mode (rather than relative to the higher-energy π -coordination modes). In addition, products that result from insertion of ethylene, $\text{HN}=\text{CH}_2$, or $\text{H}_2\text{C}=\text{O}$ can potentially interact with the metal center’s open coordination site through a C–H agostic interaction or a π -interaction via the phenyl ring (Scheme 4). For the insertion of formaldehyde and ethylene, the π -coordination mode of the (Tab)Ru(CO)(OCH₂Ph) and (Tab)Ru(CO)(CH₂CH₂Ph) products, respectively, are calculated to be marginally more stable than their corresponding C–H agostic conformers (Scheme 4), while the order of conformer stability is reversed for the product of imine insertion (Tab)Ru(CO)(N(H)CH₂Ph). All reported

(81) Bergman, R. G.; Cundari, T. R.; Gillespie, A. M.; Gunnoe, T. B.; Harman, W. D.; Klinckman, T. R.; Temple, M. D.; White, D. P. *Organometallics* **2003**, *22*, 2331–2337.

Scheme 5. Calculated Binding Free Energies (kcal/mol) of Methyleneimine, Ethylene, and Formaldehyde to $\{(\text{Tab})\text{Ru}(\text{CO})(\text{Ph})\}$



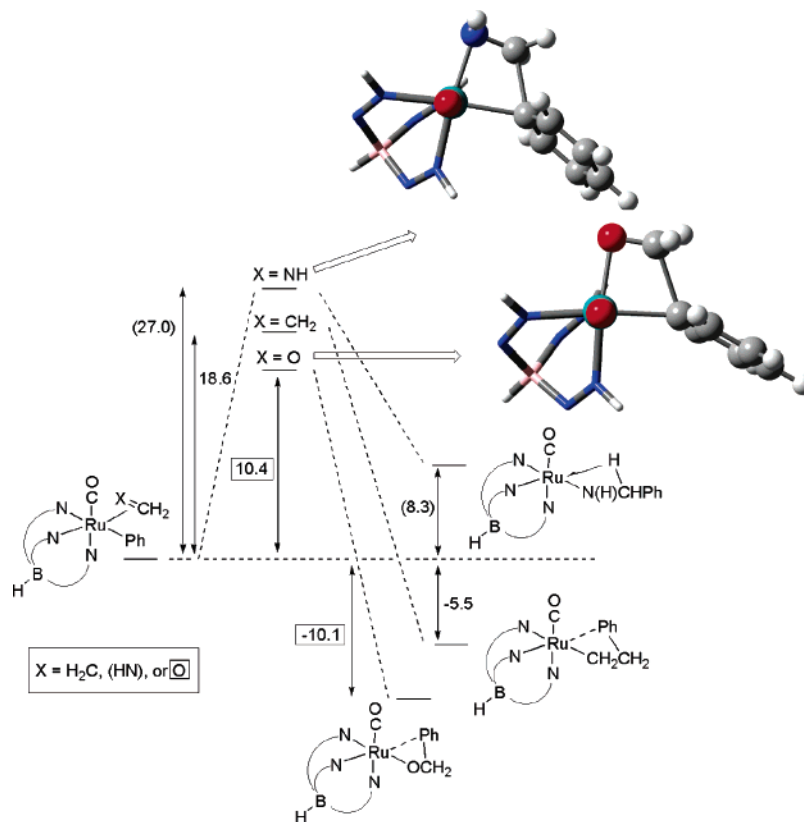
energetic data involving these products are relative to the lowest-energy coordination mode.

Computational Results for Ethylene, Methyleneimine, and Formaldehyde. To observe insertion of a substrate into the Ru–Ph bond of complex **1**, coordination to the Ru metal center is necessary. Given previous studies on TpRu(CO)(NCMe)(R) systems,^{54–56,82} ligand exchange with NCMe seems the most plausible pathway. Thus, the binding energy of the substrates to $\{\text{TpRu}(\text{CO})(\text{Ph})\}$ could play a role in possible insertion reactions. Scheme 5 shows the calculated free energy changes upon coordination of substrate to the five-coordinate, 16-electron model $\{(\text{Tab})\text{Ru}(\text{CO})(\text{Ph})\}$. According to the calculations, the relative binding free energies for the most stable σ -coordination modes are (free energy change relative to HN=CH₂ given in

parentheses): methyleneimine > ethylene (7.2 kcal/mol) > formaldehyde (13.5 kcal/mol). The relative calculated ground-state free energy changes, as well as the relative free energies of activation for the insertion of ethylene, HN=CH₂, and H₂C=O follow identical trends (Scheme 6). That is, the insertion of formaldehyde is calculated to be more favorable and more kinetically facile than ethylene or HN=CH₂.

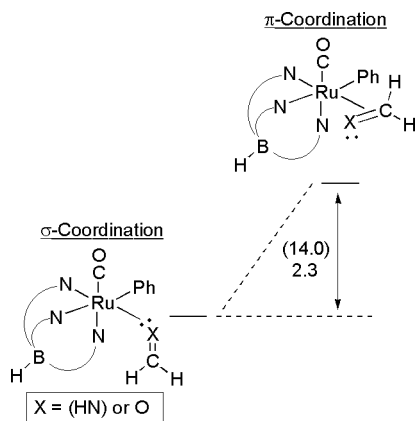
Interestingly, while the insertion of ethylene and formaldehyde are calculated to be thermodynamically favorable by –5.5 and –10.1 kcal/mol, respectively, the insertion of HN=CH₂ is calculated to be thermally disfavored by 8.3 kcal/mol. The calculated barriers for the insertion step reveal that the relative rates should follow the trend (calculated free energies of activation given in parentheses): formaldehyde (10.4 kcal/mol) > H₂C=CH₂ (18.6 kcal/mol) > methyleneimine (27.0 kcal/mol). Scheme 6 depicts the structures of the transition states for insertion of methyleneimine and formaldehyde. The transition states possess planar, four-centered active sites similar to that previously found for the insertion of ethylene into the Ru–Ph bond of $(\text{Tab})\text{Ru}(\text{CO})(\text{Ph})$.⁵⁵ The insertion transition states are best characterized as “early” on their respective reaction coordinates given the long C–C_{ipso} (≥ 1.95 Å) and short C–X (10% or less compared to their ground-state values). The isomerization of $(\text{Tab})\text{Ru}(\text{CO})(\text{Ph})(\text{L})$ (L = methyleneimine or formaldehyde) from the more stable σ -coordination mode to the π -coordination mode is calculated to be significantly less favorable for methyleneimine ($\Delta G = +14.0$ kcal/mol) than for formaldehyde ($\Delta G = +2.3$ kcal/mol), a result that is potentially exacerbated experimentally by substitution of the hydrogen

Scheme 6. Calculated Free Energies (kcal/mol) for Insertion of Ethylene, HN=CH₂, and O=CH₂ (Values for Methyleneimine Are Given in Parentheses, and the Results for the Formaldehyde Are Given in Boxes) into the Ru–Ph Bond of $\{\text{TpRu}(\text{CO})(\text{Ph})\}$ ^a



^a Data for methyleneimine and formaldehyde correspond to the starting material with the substrate in the σ -coordination mode; ethylene is π -coordinated. The β -agostic isomers for Ru–OCH₂Ph and Ru–CH₂CH₂Ph are calculated to be 2.0 and 1.3 kcal/mol, respectively, higher in free energy than the corresponding π -conformers. The β -agostic conformer for Ru–N(H)CH₂Ph is calculated to be 0.8 kcal/mol lower in free energy than the corresponding π -conformer.

Scheme 7. Calculated Free Energy Changes for Conversion of the σ -Coordination Mode to π -Coordination for (Tab)Ru(CO)(HN=CH₂)(Ph) (+14.0 kcal/mol) and (Tab)Ru(CO)(O=CH₂)(Ph) (+2.3 kcal/mol)

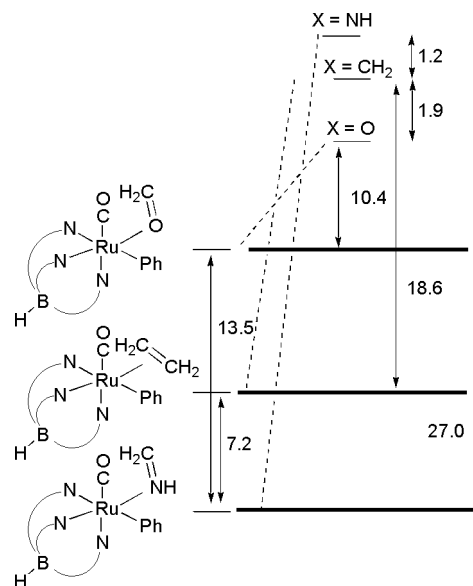


atoms on the imine with more sterically bulky groups (Scheme 7). Thus, the calculations suggest that observation of imine insertion may be kinetically inhibited by, among other possibilities, unfavorable isomerization to the π -coordination mode from the σ -coordination mode, which is attributable in part to the strong imine–Ru σ -bonding in the η^1 -coordination mode. Experimentally, the insertion of ethylene into the Ru–Ph bond of complex **1** to produce TpRu(CO)(NCMe)(CH₂CH₂Ph) has been directly observed,⁵⁵ which is consistent with the calculated favorable coordination of ethylene and relatively low free energy of activation for ethylene insertion into the Ru–Ph bond. Given that formaldehyde insertion is calculated to be thermally favorable ($\Delta G = -10.1$ kcal/mol) and calculated to proceed with a relatively low free energy of activation ($\Delta G^\ddagger = 10.4$ kcal/mol), the failure to observe insertion reactions of aldehydes or ketones when reacted with TpRu(CO)(NCMe)(Ph) is likely attributable to relatively weak coordination of the carbonyl group to the metal center and thus an inability to displace the acetonitrile ligand and/or thermodynamically favorable C–H activation and decarbonylation of the aldehyde (see below).

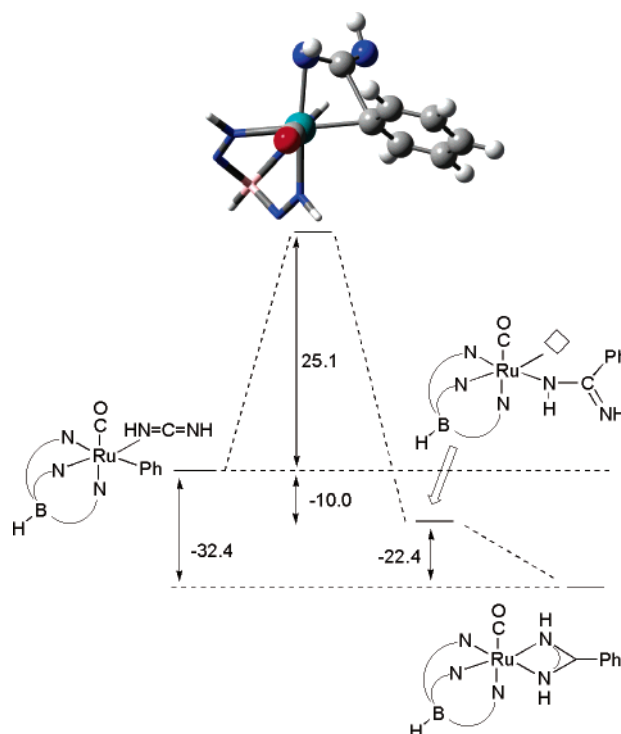
The differences in the free energies of activation for insertion of formaldehyde, ethylene, and methyleneimine are similar to the differences in ground state energies between these systems (Scheme 8). The relative energies for ground states and transition states are inversely related, with the energy differences in the transition states less pronounced than those in the ground states. The free energy changes upon coordination of ethylene and formaldehyde to (Tab)Ru(CO)(Ph), relative to the ΔG for coordination of methyleneimine, are 7.2 (ethylene) and 13.5 kcal/mol (formaldehyde). The free energies of activation of insertion into the Ru–Ph bond, relative to the ΔG^\ddagger for insertion of methyleneimine, are 8.2 (ethylene) and 16.6 kcal/mol (formaldehyde). Thus, according to the calculations, the differences in activation barrier for insertion of formaldehyde, methyleneimine, and ethylene into the Ru–Ph bond of (Tab)Ru(CO)(Ph) are likely due to differences in ground state energies of (Tab)Ru(CO)(Ph)(L) (L = formaldehyde, methyleneimine, or ethylene).

Computational Results for Carbodiimide. Scheme 9 depicts calculated free energy changes for the insertion of HN=C=NH into the Ru–Ph bond of {(Tab)Ru(CO)(Ph)} using the σ -coordination mode of the carbodiimide. The insertion of

Scheme 8. Comparison of Calculated Differences of Ground-State Free Energies and Transition States for Insertion of “L” into the Ru–Ph Bond of (Tab)Ru(CO)(Ph)(L) (L = Methyleneimine, Formaldehyde, or Ethylene)

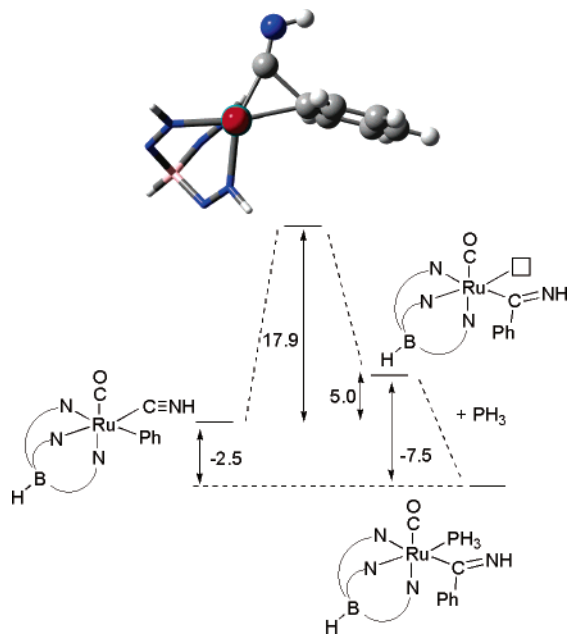


Scheme 9. Calculated Free Energies (kcal/mol) for Insertion of Carbodiimide (HN=C=NH) into the Ru–Ph Bond of {TpRu(CO)(Ph)} and Subsequent Formation of an Amidinate



carbodiimide into the Ru–Ph bond of **1** provides an interesting contrast to the insertion of imine for three reasons: (1) net carbodiimide insertion into the Ru–Ph bond of **1** has been experimentally observed, (2) the first step involves formal insertion of a C=N bond in both processes, and (3) kinetic access to insertion of a carbodiimide provides the opportunity to trap the initial insertion product via formation of a chelating amidinate ligand. In contrast to methyleneimine, the insertion of a C=N bond of HN=C=NH into the Ru–Ph bond of **1** is

Scheme 10. Calculated Free Energies (kcal/mol) for Insertion of Isonitrile into the Ru–Ph Bond of {TpRu(CO)(Ph)} and Subsequent Coordination of PH₃



calculated to be exergonic by 10.0 kcal/mol with an activation barrier of 25.1 kcal/mol (Scheme 9). Thus, although this reaction step is calculated to have a similar free energy of activation compared to insertion of the imine $\text{HN}=\text{CH}_2$, it is calculated to be substantially more favorable thermodynamically with $\Delta\Delta G = 18.3$ kcal/mol. The formation of a chelating amidinate ligand is calculated to be quite favorable with an overall change in free energy of -22.4 kcal/mol versus the η^1 product of initial carbodiimide insertion. Thus, conversion of $(\text{Tab})\text{Ru}(\text{CO})(\text{Ph})-(\eta^1\text{-HN}=\text{C}=\text{NH})$ to the amidinate complex $(\text{Tab})\text{Ru}(\text{CO})(\kappa^2\text{-N,N-HNC}(\text{Ph})\text{NH})$ is calculated to be favorable by a substantial -32.4 kcal/mol.

The computational results for methyleneimine and the parent carbodiimide suggest that the experimentally observed differences between carbodiimides (net insertions *observed*) and imines (net insertions *not observed*) may be derived from thermodynamic differences. The calculated activation barriers for the insertion of methyleneimine and the parent carbodiimide into the Ru–Ph bond of $(\text{Tab})\text{Ru}(\text{CO})(\text{Ph})$ are quite similar with $\Delta\Delta G^\ddagger = 1.9$ kcal/mol (Schemes 6 and 9). In both cases, the stable σ -coordination mode (relative to the π -coordination mode) likely contributes to the calculated substantial Gibbs free energy of activation. Furthermore, conversion of the product from carbodiimide insertion to a chelating amidinate ligand provides a significant driving force and an additional 22.4 kcal/mol of stabilization.

Computational Results for Isonitrile. Free energy changes for insertion of isonitrile into the Ru–Ph bond of $(\text{Tab})\text{Ru}(\text{CO})(\text{Ph})(\text{C}\equiv\text{NH})$ and subsequent coordination of PH_3 were calculated (Scheme 10). The initial insertion is calculated to occur with $\Delta G^\ddagger = 17.9$ kcal/mol and an unfavorable change in free energy of $\Delta G = +5.0$ kcal/mol. Coordination of PH_3 is calculated to stabilize the insertion product by -7.5 kcal/mol, providing an overall $\Delta G = -2.5$ kcal/mol for the conversion of $(\text{Tab})\text{Ru}(\text{CO})(\text{Ph})(\text{C}\equiv\text{NH})$ and PH_3 to $(\text{Tab})\text{Ru}(\text{CO})(\text{C}(\text{Ph})\text{NH})(\text{PH}_3)$. The calculations are qualitatively consistent with experimental results discussed above. For example, heating a benzene solution of $\text{TpRu}(\text{CO})(\text{CN}^i\text{Bu})(\text{Ph})$ (**5**) in the absence of phosphine results in no observed changes; however, heating

5 in the presence of PMe_3 allows observation of an equilibrium between **5**/ PMe_3 and the insertion product $\text{TpRu}(\text{CO})\{\text{C}(\text{Ph})=\text{N}^i\text{Bu}\}(\text{PMe}_3)$ (**6**).

Computational Results for Decarbonylation. Calculations reveal that aldehyde insertion into the Ru–Ph bond of $(\text{Tab})\text{Ru}(\text{CO})(\text{Ph})$ should be facile and favorable (see above). However, reaction of $\text{TpRu}(\text{CO})(\text{NCMe})(\text{Ph})$ with benzaldehyde or *p*-tolualdehyde results in decarbonylation reactions to produce benzene and $\text{TpRu}(\text{CO})_2(\text{Ar})$ ($\text{Ar} = \text{Ph}$ or *p*-tolyl). The net decarbonylation reactions likely proceed by cleavage of an aldehyde C–H bond, C–H bond formation with the phenyl ligand (to produce benzene), and deinsertion of CO from an acyl ligand. We have previously reported that fragments of the type $\{\text{TpRu}(\text{CO})(\text{R})\}$ can react with aromatic C–H bonds to produce R–H and $\{\text{TpRu}(\text{CO})(\text{Ar})\}$ systems with calculated transition states that involve concerted C–H bond breaking and R–H bond formation.^{55,56} Calculations reveal a similar transition state for C–H activation of formaldehyde by $(\text{Tab})\text{Ru}(\text{CO})(\text{Ph})$ (Scheme 11). The C–H activation transition state for formaldehyde is structurally similar to related σ -bond metathesis-type transition states in which the metal is within bonding distance with the transannular hydrogen atom (previously referred to as oxidative hydrogen migration):⁴⁶ planar, four-centered active site with obtuse angle at the hydrogen being transferred (H_i) and a near covalent Ru– H_i distance (1.69 Å). The calculated ΔG^\ddagger for aldehyde C–H activation is relatively small (18.6 kcal/mol) compared with analogous calculated value for benzene C–H activation (21.2 kcal/mol) by $(\text{Tab})\text{Ru}(\text{CO})(\text{Me})$ but is larger than the corresponding value for furan C–H activation (17.4 kcal/mol).^{55,56} These results suggest that if decarbonylation can be avoided, catalysts for the addition of aldehyde C–H bonds across olefin C=C bonds might be possible with closely related Ru(II) systems. The calculations indicate that aldehyde C–H activation has a more substantial activation barrier than insertion of the C=O bond into the Ru–Ph bond; however, the initial products of aldehyde C–H activation (benzene and an η^2 -formyl complex) are more stable than the product of C=O insertion by 3.2 kcal/mol (Scheme 11). Furthermore, the decarbonylation step to produce $(\text{Tab})\text{Ru}(\text{CO})_2(\text{H})$ is highly favorable and is calculated to produce products that are 46.9 kcal/mol more stable than starting materials $\{\text{Tab}\text{Ru}(\text{CO})(\text{Ph})$ and $\text{CH}_2\text{O}\}$. Thus, the calculations suggest that carbonyl insertion is kinetically feasible but is likely difficult to observe due to facile and thermally favorable decarbonylation.

Calculated Bond Dissociation Energies. We have calculated the energetics for insertion of ethylene, formaldehyde, methylene imine, $\text{HN}=\text{C}=\text{NH}$, and isonitrile into a Ru(II) phenyl bond. To probe the possible correlation of C=X/C–X BDE on insertion parameters, the BDEs of these substrates and their hydrogenated counterparts have been calculated (Table 2). Comparing either the calculated ΔH for insertion or the ΔH^\ddagger for insertion with the ΔBDE for the entire series does not reveal any correlation. For example, the change in calculated N–C BDE upon conversion of $\text{H}_2\text{C}=\text{NH}$ (155.2 kcal/mol) to $\text{H}_3\text{C}-\text{NH}_2$ (81.9 kcal/mol) results in the least unfavorable ΔBDE (73.3 kcal/mol) among the series methyleneimine, ethylene ($\Delta\text{BDE} = 84.3$ kcal/mol), and formaldehyde ($\Delta\text{BDE} = 87.0$ kcal/mol), yet insertion of methyleneimine is calculated to be least favorable ($\Delta H_{\text{insertion}} = +7.1$ kcal/mol) and to possess the largest ΔH^\ddagger for insertion (25.1 kcal/mol). However, the ΔBDE for $\text{HN}=\text{C}=\text{NH}$ is calculated to be substantially more favorable when compared to the ΔBDE of methyleneimine ($\Delta\Delta\text{BDE} = 18.3$ kcal/mol) with the calculated $\Delta\Delta H_{\text{insertion}} = 18.4$ kcal/mol.

Scheme 11. Calculated Free Energies for C–H Activation of Formaldehyde and C=O Insertion into Ru–C_{ipso} Bond by (Tab)Ru(CO)(Ph)

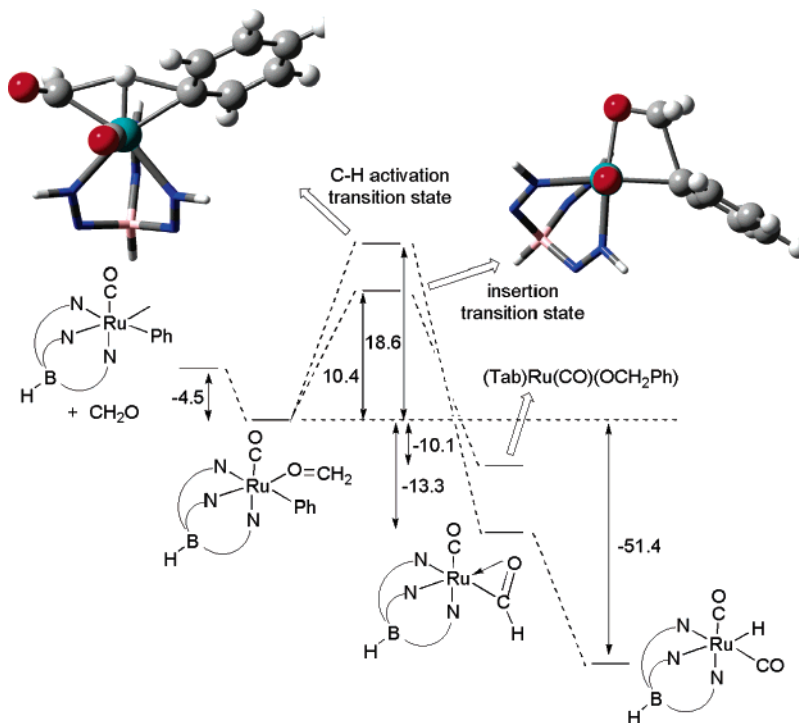


Table 2. Calculated BDEs for Ethylene, HN=C=NH, Formaldehyde, Methyleneimine, Isonitrile, and the Products of Hydrogenation^a

substrate	BDE	substrate	BDE	Δ BDE	$\Delta H_{\text{insertion}}$	$\Delta H_{\text{insertion}}^{\ddagger}$
H ₂ C=O	176.9	H ₃ C–OH	89.9	87.0	–12.7	7.5
H ₂ C=CH ₂	171.8	H ₃ C–CH ₃	87.5	84.3	–5.8	17.7
HN=C=NH	151.0 ^b	H ₂ N–C(H)=NH	96.0	55.0	–11.3	22.3
H ₂ C=NH	155.2	H ₃ C–NH ₂	81.9	73.3	+7.1	25.1
C≡NH	208.1	H ₂ C=NH	155.2	52.8	+3.7	16.6

^a Bond dissociation enthalpies (kcal/mol) calculated using a modified G3 method employing correlation consistent basis sets that has been shown to yield an average accuracy in calculated thermodynamics of ± 1 kcal/mol (DeYonker, N. J.; Cundari, T. R.; Wilson, A. K. *J. Chem. Phys.*, in press). ^b Average bond dissociation enthalpy for C=N; calculated from HN=C=NH \rightarrow C (3 P) + 2 NH (3 Π).

Thus, the calculated N–C BDE of H₂N–C(H)=NH (96.0 kcal/mol) being larger than that of H₃C–NH₂ (81.9 kcal/mol, see Table 2) provides a possible rationalization for the calculated $\Delta H_{\text{insertion}}$ for HN=C=NH being exothermic while that of HN=CH₂ is endothermic. While BDEs obviously impact the likelihood of insertion reactions occurring, establishing general trends based on simple comparison of BDEs is not likely to be possible.

Summary and Conclusions. The combination of experimental and computational studies on insertion of C–X multiple bonds into the Ru(II) phenyl bond of the fragment {TpRu(CO)(Ph)} leads us to the following conclusions.

(1) The scarcity of direct observation of insertion of C–N or C–O multiple bonds into M–H, M–R, or M–Ar bonds is not attributable *in general* to an inherently large activation barrier due to the large BDEs of C–N/C–O multiple bonds.

(2) For TpRu(CO)(NCMe)(Ph), the failure to observe imine insertions is proposed to arise from a substantial activation barrier (attributable, at least in part, to strong η^1 -binding of the imine) in combination with an unfavorable change in free energy for formation of the insertion product.

(3) The failure to observe insertion of aldehyde C=O bonds is likely due to the highly favorable and kinetically accessible aldehyde C–H activation/decarbonylation.

(4) Insertion of isonitrile into the Ru–Ph bond of TpRu(CO)(CN^tBu)(Ph) (**5**) is thermally disfavored, and the addition/

coordination of PMe₃ provides a driving force to observe the *kinetically accessible* insertion by trapping the insertion product.

(5) Similar to imines, the insertion of carbodiimides is likely to proceed with a relatively high activation barrier; however, the insertion is overall thermodynamically favorable and the formation of chelating amidinate ligand provides a large enthalpic gain that allows trapping through formation of a very stable product.

(6) Given the calculated weak binding of formaldehyde to the model (Tab)Ru(CO)(Ph) fragment, the failure to experimentally observe insertion of ketones into the Ru–Ph bond of complex **1** could be attributable to the difficulty in coordinating the ketone substrates in a dihapto-coordination mode.

(7) For systems of the type {TpRu(L)(R)} that have been demonstrated to activate C–H bonds, catalytic reactions that involve the hydroarylation of C–X multiple bonds are potentially viable for some systems (e.g., carbodiimides and isonitriles) if conditions can be found for release of the product of insertion (via C–H activation of an external substrate). Extension of such transformations to other substrates (e.g., aldehydes, ketones, imines) will require tuning to overcome the limitations identified herein.

Experimental Section

General Methods. All reactions and procedures were performed under anaerobic conditions in a nitrogen-filled glovebox or using standard Schlenk techniques. Glovebox purity was maintained by periodic nitrogen purges and monitored by an oxygen analyzer $\{O_2(g) < 15 \text{ ppm for all reactions}\}$. Photolysis experiments were performed using a 450 W power supply, 450 W lamp, and a quartz cooling jacket filled with flowing water. Acetonitrile was purified by passage through two columns of activated alumina followed by distillation from CaH_2 . Dichloromethane and hexanes were purified by passage through two columns of activated alumina. Benzene, diethyl ether, pentane, tetrahydrofuran, and toluene were purified by distillation from sodium/benzophenone. Acetone- d_6 , CD_3CN , C_6D_6 , $CDCl_3$, and $C_6D_5CD_3$ were degassed via three freeze-pump-thaw cycles and stored over activated 4 Å sieves. 1H and ^{13}C NMR spectra were obtained on either a Varian Mercury 300 MHz or Varian Mercury 400 MHz spectrometer (operating frequencies for ^{13}C NMR are 75 and 100 MHz, respectively) and referenced against tetramethylsilane using residual proton signals (1H NMR) or the ^{13}C resonances of the deuterated solvent (^{13}C NMR). Resonances due to the Tp ligand are listed by chemical shift and multiplicity only (all coupling constants for the Tp ligand are 2 Hz). ^{31}P NMR spectra were obtained on a Varian Mercury 400 MHz (operating frequency = 161 MHz) spectrometer and referenced against external 85% H_3PO_4 . Unless otherwise noted, NMR spectra were acquired at room temperature. IR spectra were obtained on a Mattson Genesis II spectrometer as thin films on a KBr plate or in solution using a KBr solution cell. Elemental analyses were performed by Atlantic Microlabs, Inc. Synthetic and characterization details of $TpRu(CO)(NCMe)(Ph)$ (**1**) and $TpRu(CO)(NCMe)(OTf)$ have been previously reported.^{55,82} The carbodiimides, N,N' -di-*n*-hexylcarbodiimide and N,N' -diphenylcarbodiimide, were prepared by a procedure reported for N,N' -di-*n*-hexylcarbodiimide.⁸³ Benzaldehyde and *p*-toluolaldehyde were passed through a plug of activated neutral alumina prior to use. Acetone was stirred over activated 4 Å sieves prior to use, and acetophenone was purified by fractional distillation under reduced pressure from P_2O_5 . All other reagents were used as purchased from commercial sources.

$TpRu(CO)\{N,N-(Ph)NC(Ph)N(Ph)\}$ (2**).** A thick-walled pressure tube was charged with **1** (0.246 g, 0.535 mmol) and THF (18 mL). To the colorless solution was added N,N' -diphenylcarbodiimide (0.372 g, 1.94 mmol) in THF (2 mL), and the mixture was heated in an oil bath to 90 °C for 48 h during which time the solution changed from colorless to yellow. The volatiles were removed under reduced pressure to produce a yellow oil. A precipitate formed upon stirring the oil in pentane for 24 h. The solid was collected by vacuum filtration, washed with additional pentane, and dried in vacuo (0.129 g, 39% yield). IR (KBr): $\nu_{CO} = 1937 \text{ cm}^{-1}$. 1H NMR ($CDCl_3$, δ): 8.09, 7.81, 7.64, 7.48 (6H, 1:1:2:2 ratio, each a d, Tp CH 3/5 position), 7.22–7.17 (5H, overlapping m's, phenyl CH), 6.98–6.93 (5H, overlapping m's, phenyl CH), 6.83–6.81 (2H, m, phenyl CH), 6.54–6.52 (3H, overlapping m's, phenyl CH), 6.37, 6.10 (3H, 1:2 ratio, each a t, Tp CH 4 position). $^{13}C\{^1H\}$ NMR ($CDCl_3$, δ): 202.8 (Ru-CO), 170.1 (NCN), 147.3, 145.6, 139.0, 135.4, 135.2, 129.3, 129.2, 128.5, 128.1, 124.6, 122.0 (phenyl and Tp 3/5 positions, one resonance is absent likely due to coincidental overlap), 105.8, 105.5 (Tp 4 positions). Anal. Calcd for $C_{29}H_{25}BN_8ORu$: C, 56.78; H, 4.11; N, 18.27. Found: C, 56.71; H, 3.94; N, 18.26.

$TpRu(CO)\{N,N-(hx)NC(Ph)N(hx)\}$ (3**).** A thick-walled pressure tube was charged with **1** (0.187 g, 0.405 mmol) and THF (18 mL). To the colorless solution was added N,N' -di-*n*-hexylcarbodiimide (0.398 g, 1.89 mmol) in THF (2 mL), and the mixture was heated in an oil bath to 90 °C for 72 h during which time the

solution changed from colorless to yellow. The volatiles were removed under reduced pressure to produce a yellow oil. The mixture was purified using column chromatography on silica gel, eluting with neat toluene. The product eluted as a light green band. The toluene was removed under reduced pressure to produce a yellow-green oil. The product is highly soluble in all common organic solvents, and all attempts at isolation of a solid failed. The oil was isolated and dried in vacuo (0.149 g, 58% yield). IR (KBr): $\nu_{CO} = 1929 \text{ cm}^{-1}$. 1H NMR ($CDCl_3$, δ): 7.86, 7.77, 7.64, 7.63 (6H, 1:1:2:2 ratio, each a d, Tp CH 3/5 position), 7.44–7.41 (2H, m, phenyl CH), 7.32–7.25 (3H, overlapping m's, phenyl CH), 6.32, 6.13 (3H, 1:2 ratio, each a t, Tp CH 4 position), 2.91–2.65 (4H, m, $-NCH_2$), 1.36–1.01 (16H, overlapping br m's, $-CH_2-$), 0.79 (6H, t, $^3J_{HH} = 6.6 \text{ Hz}$, $-CH_3$). $^{13}C\{^1H\}$ NMR ($CDCl_3$, δ): 203.5 (Ru-CO), 175.0 (NCN), 145.0, 138.8, 135.1, 134.7, 132.2, 128.8, 128.4, 128.3 (phenyl and Tp 3/5 positions), 105.7, 104.9 (Tp 4 positions), 48.4, 32.5, 32.0, 26.9, 22.9 (CH_2), 14.4 (CH_3). Anal. Calcd for $C_{28}H_{41}BN_8ORu$: C, 54.46; H, 6.69; N, 18.14. Found: C, 54.46; H, 6.65; N, 18.13.

$TpRu(CO)\{N,O-(Me)NC(Me)O\}$ (4**).** A thick-walled pressure tube was charged with **1** (0.203 g, 0.441 mmol) and THF (15 mL). To the colorless solution was added *N*-methylacetamide (0.175 mL, 2.29 mmol) in THF, and the mixture was heated in an oil bath to 90 °C for 24 h during which time the solution changed from colorless to yellow. The volatiles were removed under reduced pressure to produce a yellow oil that was dried in vacuo. Attempts to separate the excess *N*-methylacetamide from **4** were not successful. For example, complex **4** decomposes on solid-supports constructed from silica gel, activated alumina, or deactivated alumina. Attempts at recrystallization from multiple solvents (including mixtures) failed to produce pure material. Efforts to sublime the *N*-methylacetamide under reduced pressure (~ 30 °C and ~ 20 mTorr) resulted in the decomposition of **4**. Heating a 1:1 mixture of **1** and *N*-methylacetamide resulted in the decomposition of **1**. Last, a mixture of the previously reported $TpRu(CO)(NCMe)(OTf)$ and lithium *N*-methylacetamidate were reacted in attempts to independently synthesize **4**; however, no reaction was observed at ambient conditions and decomposition was observed at elevated temperatures. Since **4** could not be separated from *N*-methylacetamide, characterization data include only IR and 1H NMR spectroscopy. IR (KBr): $\nu_{CO} = 1944 \text{ cm}^{-1}$. 1H NMR ($CDCl_3$, δ): 7.77, 7.42, 7.57, 7.48 (4H total, 1:1:1:1 ratio, each a d, Tp CH 3/5 position), 7.63 (2H total, overlapping d's, Tp CH 3/5 position), 6.34, 6.15, 6.13 (3H total, 1:1:1 ratio, each a t, Tp CH 4 position), 2.83 (3H total, s, $-CH_3$), 1.92 (3H total, s, $-CH_3$).

$TpRu(CO)(CN^tBu)(Ph)$ (5**).** A colorless solution of **1** (0.233 g, 0.507 mmol) and *tert*-butylisocyanide (0.30 mL, 2.6 mmol) in THF (20 mL) was heated in an oil bath to 90 °C for 21 h. After the heating, the volatiles were removed in vacuo to produce a colorless oil. The oil was dissolved in dichloromethane and purified by column chromatography on silica gel, eluting with neat dichloromethane. The product eluted as a light yellow band. The volatiles were removed under reduced pressure to produce a white solid. To the resulting white solid was added hexanes, and the mixture was stored overnight at -20 °C. The white solid was collected by vacuum filtration, washed with pentane, and dried in vacuo (0.085 g, 33% yield). IR (KBr): $\nu_{CO} = 1952 \text{ cm}^{-1}$ and $\nu_{CN} = 2143 \text{ cm}^{-1}$. 1H NMR ($CDCl_3$, δ): 7.67 (4H, overlapping d's, Tp CH 3/5 position), 7.34, 7.23 (2H, 1:1 ratio, each a d, Tp CH 3/5 position), 6.87–6.90 (5H, m, phenyl CH), 6.21 (1H, t, Tp CH 4 position), 6.14 (2H, overlapping t's, Tp CH 4 position), 1.51 (9H, s, CH_3). $^{13}C\{^1H\}$ NMR ($CDCl_3$, δ): 203.6 (Ru-CO), 161.4 (Ru-phenyl *ipso*), 144.2, 143.2, 143.0, 142.2, 134.7, 134.6, 134.5, 125.8, 121.1 (phenyl, Tp 3/5 positions, and Ru- CN^tBu), 105.5, 105.4, 105.3 (Tp 4 positions), 57.5 $\{C(CH_3)_3\}$, 31.5 $\{C(CH_3)_3\}$. Anal. Calcd for $C_{21}H_{24}BN_7ORu$: C, 50.21; H, 4.82; N, 19.52. Found: C, 50.21; H, 4.99; N, 19.23.

(83) Shibayama, K.; Seidel, S. W.; Novak, B. M. *Macromolecules* **1997**, *30*, 3159–3163.

Sample Procedure for Reaction of TpRu(CO)(CN'Bu)(Ph) (5) with PMe₃ to Produce TpRu(CO)(PMe₃){C(Ph)=N(Bu)} (6). A J-Young NMR tube was charged with **1** (0.029 g, 0.057 mmol) and C₆D₆ (1.0 mL). To the colorless solution was added PMe₃ (0.025 mL, 0.28 mmol). The mixture was heated to 100 °C and monitored periodically by ¹H NMR spectroscopy over the course of 24 h at which time it was determined that the system had reached equilibrium between **5** and complex **6**. IR (thin film on KBr) analysis revealed complex **5** ($\nu_{\text{CO}} = 1952 \text{ cm}^{-1}$ and $\nu_{\text{CN}} = 2143 \text{ cm}^{-1}$) and a new complex assigned as TpRu(CO)(PMe₃){C(Ph)=N(-Bu)} (**6**) with a $\nu_{\text{CO}} = 1927 \text{ cm}^{-1}$. ¹H NMR (C₆D₆, δ): 8.75, 7.56, 6.23 (3H, 1:1:1 ratio, each a d, Tp CH 3/5 position), 6.81 (1H, tt, ³J_{HH} = 7 Hz and ⁴J_{HH} = 1 Hz, phenyl *para*-CH), 6.60 (1H, dt, ³J_{HH} = 7 Hz and ⁴J_{HH} = 1 Hz, phenyl *meta*-CH), 5.95 (1H, br dd, ³J_{HH} = 7 Hz and ⁴J_{HH} = 1 Hz, phenyl *ortho*-CH), other Tp CH 3/5 and phenyl CH resonances overlap with resonances due to complex **5**, 6.11, 5.81, 5.59 (3H, 1:1:1 ratio, each a t, Tp CH 4 position), 1.27 (9H, d, ³J_{HP} = 10 Hz, P(CH₃)₃), 1.21 (9H, s, CH₃). ³¹P{¹H} NMR (C₆D₆, δ): 11.0 (PMe₃). The volatiles were removed in vacuo (including all PMe₃), and the resulting oil was taken up in C₆D₆ (1.0 mL). Heating this solution to 100 °C for 72 h resulted in conversion predominantly to complex **5** and free trimethylphosphine, as determined by ¹H NMR, ³¹P{¹H} NMR, and IR spectroscopy.}}}}}}}

TpRu(CO)(PMe₃)(Ph) (7). A colorless solution of **1** (0.208 g, 0.451 mmol) and trimethylphosphine (0.20 mL, 2.3 mmol) in THF (20 mL) was heated in an oil bath to 90 °C for 24 h. After the heating, the volatiles were removed in vacuo to produce a colorless oil. The oil was dissolved in dichloromethane (2 mL), and pentane (15 mL) was added. The resulting white solid was stored for ~12 h at -20 °C, collected by vacuum filtration, washed with cold pentane, and dried in vacuo (0.095 g, 43% yield). IR (KBr): $\nu_{\text{CO}} = 1928 \text{ cm}^{-1}$. ¹H NMR (CDCl₃, δ): 7.75, 7.71, 7.43, 7.15 (4H, 1:1:1:1 ratio, each a d, Tp CH 3/5 position), 7.61 (2H, overlapping d's, Tp CH 3/5 position), 7.03–7.00 (2H, m, phenyl CH), 6.89–6.83 (3H, overlapping m's, phenyl CH), 6.23 (2H, overlapping t's, Tp CH 4 position), 6.05 (1H, t, Tp CH 4 position), 1.34 (9H, d, P(CH₃)₃, ²J_{HP} = 9 Hz). ¹³C{¹H} NMR (CDCl₃, δ): 206.2 (d, ²J_{CP} = 18 Hz, Ru-CO), 165.2 (d, ²J_{CP} = 13 Hz, Ru-phenyl *ipso*), 144.0, 143.0, 142.9, 142.8, 142.6, 142.5, 135.2, 135.0, 134.3, 125.6, 120.6 (phenyl, Tp 3/5 positions), 105.5, 105.2 (Tp 4 positions), 31.5 (d, ¹J_{CP} = 30 Hz, P(CH₃)₃). ³¹P{¹H} NMR (CDCl₃, δ): 12.7 (PMe₃). Anal. Calcd for C₁₉H₂₄BN₆OPRu: C, 46.08; H, 4.88; N, 16.97. Found: C, 45.64; H, 5.07; N, 16.70.}}}}

TpRu(CO)₂(Ph) (8). A thick-walled reaction vessel was charged with **1** (0.216 g, 0.467 mmol) and THF (12 mL). To the colorless solution was added benzaldehyde (1.0 mL, 9.9 mmol), and the mixture was heated in an oil bath to 90 °C for 48 h. The volatiles were removed in vacuo to leave a light green oil. The complex was separated from the benzaldehyde by flash chromatography on silica gel, eluting with dichloromethane to yield a light green solution. The eluent was collected and reduced to dryness in vacuo, and the resulting solid was stirred in hexanes. The white solid was collected by vacuum filtration and dried in vacuo (0.114 g, 54% yield). IR and ¹H NMR spectroscopy of crude reaction products revealed only complex **8**. IR (KBr): $\nu_{\text{CO}} = 2041, 1973 \text{ cm}^{-1}$. ¹H NMR (CDCl₃, δ): 7.77, 7.34 (3H, 1:2 ratio, each a d, Tp CH 3/5 position), 7.73 (3H, overlapping d's, Tp CH 3/5 position), 6.26 (5H, overlapping m's, phenyl CH), 6.28, 6.21 (3H, 2:1 ratio, each a t, Tp 4 CH position). ¹³C{¹H} NMR (CDCl₃, δ): 199.7 (Ru-CO), 154.1 (Ru-phenyl *ipso*), 144.1, 143.9, 141.8, 135.2, 135.1, 126.8 (phenyl and Tp 3/5 positions, one resonance absent most likely due to coincidental overlap), 106.2, 106.0 (Tp 4 position). Anal. Calcd for C₁₇H₁₅BN₆O₂Ru: C, 45.61; H, 3.38; N, 18.79. Found: C, 45.62; H, 3.38; N, 18.71.

TpRu(CO)₂(*p*-tolyl) (9). The procedure used was similar to that for complex **8** (with the exception that the heating period was 24

h) using **1** (0.229 g, 0.500 mmol), THF (20 mL), and *p*-tolualdehyde (0.25 mL, 2.1 mmol). Complex **9** was isolated in 26% yield (0.058 g). IR and ¹H NMR spectroscopy of crude reaction products revealed only complex **9**. IR (KBr): $\nu_{\text{CO}} = 2039, 1971 \text{ cm}^{-1}$. ¹H NMR (CDCl₃, δ): 7.74, 7.37 (3H, 1:2 ratio, each a d, Tp CH 3/5 position), 7.70 (3H, overlapping d's, Tp CH 3/5 position), 6.82 (4H, br s, phenyl CH), 6.27, 6.19 (3H, 1:2 ratio, each a t, Tp CH 4 position), 2.27 (3H, s, -CH₃). Variable-temperature NMR studies showed that the broad singlet due to the aryl hydrogens begins to deconvolve at -20 °C to produce two resonances that are not fully resolved at -60 °C. ¹³C{¹H} NMR (CDCl₃, δ): 199.8 (Ru-CO), 149.2 (Ru-phenyl *ipso*), 144.1, 143.9, 141.5, 135.2, 135.1, 131.9, 127.9 (phenyl and Tp 3/5 positions), 106.0 (Tp 4 position, overlap of resonances), 21.1 (*p*-tolyl-CH₃). Anal. Calcd for C₁₇H₁₅BN₆O₂Ru(C₅H₁₂)_{0.28} (Note: A ¹H NMR spectrum of the analysis sample indicated the presence of pentane in a 1:3.57 molar ratio with complex **9**; a ¹H NMR spectrum of **9** is included in the Supporting Information): C, 48.40; H, 4.26; N, 17.46. Found: C, 48.55; H, 4.24; N, 17.46.

Reaction of TpRu(CO)(NCMe)(Ph) (1) with *N,N*-Dimethylacetamide. A screw-cap NMR tube was charged with a solution of **1** (0.037 g, 0.081 mmol) in C₆D₆ (1.0 mL). To the colorless solution was added *N,N*-dimethylacetamide (0.075 mL, 0.81 mmol). The mixture was heated to 90 °C and monitored periodically by ¹H NMR spectroscopy over the course of 24 h. Analysis by NMR spectroscopy showed decomposition of the starting Ru complex (**1**) to NMR-silent materials without the observation of new diamagnetic Ru systems.

Attempted Insertion of Isonitrile of TpRu(CO)(CN'Bu)(Ph) (5). Method A (Thermolysis). A screw-cap NMR tube was charged with a solution of **5** (0.010 g, 0.020 mmol) in either NCCD₃ or C₆D₆ (0.7 mL). The colorless solution was heated to 100 °C and monitored periodically by ¹H NMR spectroscopy over the course of 24 h. Analysis by NMR spectroscopy showed no evidence of reaction.

Method B (Photolysis). A screw-cap NMR tube was charged with a solution of **5** (0.010 g, 0.020 mmol) in either NCCD₃ or C₆D₆ (0.7 mL). The colorless solution was photolyzed with short-wavelength UV light and monitored periodically by ¹H NMR spectroscopy over the course of 3 h. Analysis by NMR spectroscopy showed decomposition of **5** to NMR-silent materials without observation of a new diamagnetic Ru system.

Equilibrium Studies for the Reversible Conversion of TpRu(CO)(CN'Bu)(Ph) (5) to TpRu(CO)(PMe₃){C(Ph)=N(Bu)} (6). A representative experiment for the determination of K_{eq} for the reaction of **5** and PMe₃ to produce complex **6** is given. A stock solution consisting of **5** (0.069 g, 0.14 mmol), C₆D₅CD₃ (toluene-*d*₈) (4.0 mL), and PMe₃ (0.012 mL, 0.14 mmol) was prepared. Ferrocene (0.006 g, 0.0325 mmol) was added as an internal standard. The solution was equally partitioned between four J-Young NMR tubes. The solutions were separately heated to 80, 90, 100, and 110 °C. The progress of each reaction was monitored periodically by ¹H NMR spectroscopy until equilibrium was established. The relative concentrations of **5**, PMe₃, and **6** were determined by integration of ¹H NMR spectra. The same procedure was repeated in two additional experiments with variable concentrations of PMe₃ (2 and 5 equiv based on **5**).

Reactivity of TpRu(CO)(NCMe)(Ph) with Selected Ketones and Imines. Reaction of **1** with acetone, acetophenone, *N*-benzylideneaniline, or *N*-benzylidenemethylamine resulted in the isolation of NMR-silent Ru products. These reactions were monitored by ¹H NMR spectroscopy in an effort to observe insertion products (intermediates) that may decompose.

Acetone. To a screw-cap NMR tube was added a solution of **1** (0.010 g, 0.022 mmol) in acetone-*d*₆ (1.0 mL). The mixture was heated to 60 °C and monitored periodically by ¹H NMR spectroscopy over the course of 24 h. Analysis by NMR spectroscopy

showed decomposition of the starting Ru complex **1** to NMR-silent materials without evidence of new diamagnetic Ru systems.

Acetophenone. To a screw-cap NMR tube was added a solution of **1** (0.015 g, 0.033 mmol) and acetophenone (0.005 mL, 0.043 mmol) in C₆D₆ (1.0 mL). The mixture was heated to 90 °C and monitored periodically by ¹H NMR spectroscopy over the course of 24 h. Analysis by NMR spectroscopy showed decomposition of the starting Ru complex **1** to NMR-silent materials without evidence of new diamagnetic Ru systems.

N-Benzylideneaniline. To a screw-cap NMR tube was added a solution of **1** (0.011 g, 0.024 mmol) and *N*-benzylideneaniline (0.004 g, 0.022 mmol) in C₆D₆ (1.0 mL). The mixture was heated to 90 °C and monitored periodically by ¹H NMR spectroscopy over the course of 24 h. Analysis by NMR spectroscopy showed decomposition of the starting Ru complex **1** to NMR-silent materials without evidence of new diamagnetic Ru systems.

N-Benzylidenemethylamine. To a screw-cap NMR tube was added a solution of **1** (0.016 g, 0.035 mmol) and *N*-benzylidenemethylamine (0.005 mL, 0.040 mmol) in C₆D₆ (1.0 mL). The mixture was heated to 90 °C and monitored periodically by ¹H NMR spectroscopy over the course of 24 h. Analysis by NMR spectroscopy showed decomposition of the starting Ru complex **1** to NMR-silent materials without evidence of new diamagnetic Ru systems.

Computational Methods. Calculations employ the Gaussian98 and Gaussian03 packages.⁸⁴ B3LYP⁸⁵ calculations were performed

(84) Frisch, M. J. et al., Gaussian 03, Revision C.02, Gaussian Inc., Wallingford, CT, 2004.

(85) (a) Becke, A. D. *Phys. Rev.* **1998**, A38, 3098–3100. (b) Lee, C.; Yang, W.; Parr, R. G. *Phys. Rev.* **1998**, B37, 785–789.

on the experimental models described in the text. Ruthenium and the main group elements were described with the Stevens (CEP-31G) relativistic effective core potentials and valence basis sets.⁸⁶ The valence basis sets of main group elements (boron, carbon, nitrogen, oxygen) were augmented with a d polarization function ($\xi_d = 0.80$). For Ru complexes, the geometry was optimized for the singlet spin state, and all the geometries were fully optimized without any symmetry constraints.

Acknowledgment. T.R.C. and T.B.G. acknowledge the Office of Basic Energy Sciences, United States Department of Energy for support of this research through Grants No. DE-FG02-03ER15387 and DE-FG02-03ER15490, respectively. T.B.G. also acknowledges support by the Alfred P. Sloan Foundation (Research Fellowship) for financial support. J.P.L. thanks GlaxoSmithKline for support through a graduate fellowship. Calculations employed the UNT computational chemistry resource, for which T.R.C. acknowledges the NSF for support through Grant No. CHE-0342824. The CASCaM facility at UNT is supported by the United States Department of Education.

Supporting Information Available: Full details of computational studies and details of X-ray data collection and structure solution for complex **9**. This material is available free of charge via the Internet at <http://pubs.acs.org>.

OM050967H

(86) Stevens, W. J.; Krauss, M.; Basch, H.; Jasien, P. G. *Can. J. Chem.* **1992**, 70, 612–630.